JOURNAL OF MATERIALS SCIENCE 13 (1978) 2429–2440

Interfacial slip and damping in fibre reinforced composites

D. J. NELSON, J. W. HANCOCK
Department of Mechanical Engineering, University of Glasgow, UK

The effect of interfacial slip on the stress–strain properties of a rubbery polymer reinforced with short fibres is discussed with particular reference to hysteresis. The amount of energy dissipated by interface sliding and by the viscoelastic response of the matrix is calculated in the light of a simple model. This is compared with the dynamic properties of the composites, both with a view to designing composites with a useful combination of stiffness and damping, and also with the possibility of evaluating the integrity of the fibre–matrix interface from dynamic measurements.

1. Introduction

The possibility of developing fibre reinforced materials which exhibit significant amounts of damping combined with sufficient stiffness for practical use has been discussed by McLean and Read [1]. Two sources of damping or energy loss may be considered; firstly viscoelastic energy dissipation by the matrix, and secondly frictional energy loss caused by sliding at the fibre–matrix interface. Both of these effects are shown most markedly in discontinuous fibre composites in which high shear stresses are developed near the fibre–matrix interface. Although at a given volume fraction of fibres the highest stiffness is obtained from continuous fibres, the damping produced by such a composite is necessarily low, as shown by Hashin [2]. When a composite with short fibres is subject to a small tensile strain cycle the matrix near the fibre undergoes a large shear strain cycle, due to the stress concentration, and may thus produce a significant viscoelestic energy loss. Alternatively, the high shear stresses may cause the fibre–matrix interface to fail so that energy is dissipated by friction as the matrix slides over the fibres. In all cases of practical interest the fibres themselves are very much stiffer than the matrix and have low damping characteristics so that the energy loss from the fibres is usually negligible.

In the present work the mechanism of interfacial slip is examined as a source of damping, not only with a view to designing composites with a useful combination of damping and stiffness, but also with the possibility of quantifying fibre–matrix interface damage from dynamic hysteresis measurements [3]. Both of these require an understanding of the mechanism of viscoelastic energy loss from the matrix and of the mechanism of interfacial slip. In the first part of the work, the hysteresis and stress–strain curves of composites with and without interfacial slip are examined in the light of a simple model of slip, and this is subsequently related to the damping measurements in dynamic tests.

2. Material and test methods

The matrix used in the composites was a silicone rubber, designated "Silcoset 100", which as well as being viscoelastic could be either strongly or weakly bonded to the fibres by the use of a priming agent. Steel rods 25 mm in length and 0.4 mm in diameter were used as fibres. The composites were made in a mould consisting of a grooved steel plate into which fibres were placed at a centre-to-centre spacing of 0.94 mm and with an overlap of 12 mm between adjacent fibres. Long fibres were placed at the ends to form part of the grip, and a lamina was cast using vacuum degassed silicone rubber, and subsequently cured in air. Rod specimens 150 mm long by 6.25 mm square were fabricated by bonding strips of the lamina. The central 100 mm contained the array of short fibres and the remaining 25 mm at either end, containing the

© 1978 Chapman and Hall Ltd. Printed in Great Britain.

long fibres, was encapsulated in epoxy resin to provide a hard grip for the specimen. Specimens were also made incorporating only the end fibres for gripping, and this allowed the properties of the matrix alone to be tested.

The fibres were either strongly bonded to the matrix by the use of a priming agent, or weakly bonded by not using the primer. In addition, in order to vary the surface roughness of the fibres and the subsequent ease of sliding, some specimens were made from fibres which had been etched in dilute nitric acid.

Slow tensile tests were performed on an Instron testing machine at a strain rate of $0.07\,sec^{-1}$ using an extensometer mounted across the gauge length to monitor strain. As the properties of the fibre–matrix interface are known to be important, pull-out tests were performed on single fibres cast into cylinders of matrix, enabling a qualitative description of the condition of the fibre–matrix interface to be made.

Dynamic tests were performed on the materials in two ways; firstly in an Instron testing machine with an imposed sinusoidal strain-controlled loading at 0.83 Hz, and secondly by using the material as the spring-damper element in a one degree of freedom vibrating system resonating at about 20 Hz. In the first case the force was measured by a conventional load cell having a stiffness between one and two orders of magnitude greater than the specimens tested and a hysteretic energy loss which was negligible compared with the materials tested. The stiffness results were thus corrected for the stiffness of the load cell, although the energy lost extraneously was considered negligible. In all cases, tests were performed with a tensile mean load to prevent buckling.

Resonating tests were performed in the equipment shown in Fig. 1. This consisted of a large rectangular steel frame filled with concrete and mounted on rubber pads. The upper end of the specimen was clamped to the frame, while the lower end of the specimen was fixed to a cylindrical mass. The lower end of the mass was connected to a Ling Dynamics vibrator by a force gauge. The vibrator was driven by a beat frequency oscillator through an amplifier, and in order to maintain a constant force input the force signal was connected to the feedback circuit of the beat frequency oscillator. An accelerometer on the mass was used to monitor the vibration. A more detailed description of this equipment and the experimental details is given by Nelson [4] along with a more detailed discussion of the problems of the analysis and synthesis of non linear vibration data.

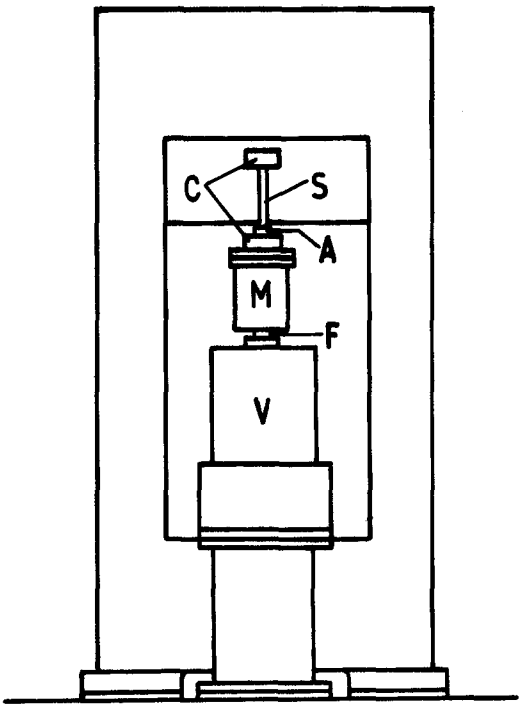

Figure 1 Schematic diagram of the equipment used in the resonating tests. The specimen is labelled S, the accelerometer A, the mass M, the force gauge F, the vibrator V and the clamps on the specimen C.

3. Results

A typical stress–strain loop of one of the composites in which the fibres were strongly bonded to the matrix is shown in Fig. 2. This material exhibited basically elastic behaviour until failure occurred by tensile failure of the matrix, there being no evidence of fibre failure or of failure of the fibre–matrix interface. A more detailed examination showed that as well as being non-linear the material exhibited hysteresis reflecting the viscoelastic behaviour of the matrix alone as shown in Fig. 3, although both the stiffness and specific damping capacity of the composites were greater than the matrix alone.

In contrast the stress–strain curves of the weakly bonded composites are shown in Figs. 4a and b and can be seen to be bi-linear. By analogy with the stress–strain curve of metals we may call the modulus transition a yield point, although in these composites it is associated with slip at the fibre–matrix interface. When the composites were

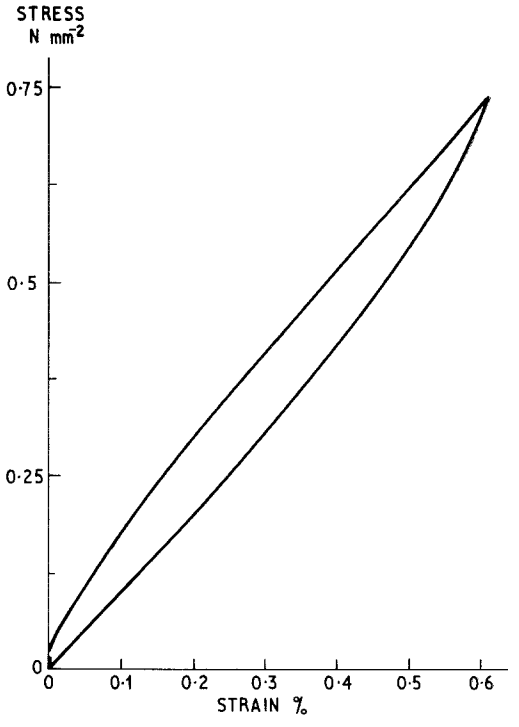

Figure 2 The stress–strain loop of a bonded composite.

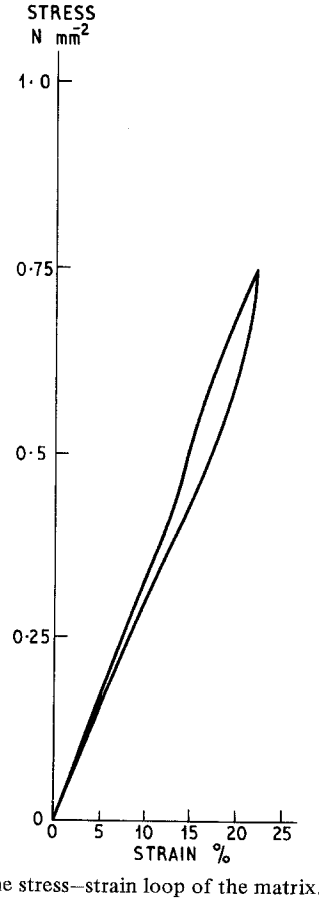

Figure 3 The stress–strain loop of the matrix.

unloaded, interfacial slip again occurred, but in the reverse direction so that the loops generally returned to the origin except for very large strain amplitude cycles. During unloading many specimens exhibited the curious phenomenon of a negative modulus, in that as the specimen became shorter as the tensile load borne by the specimen increased. This feature occurred most markedly in the specimens containing etched fibres. Such specimens also showed a marked yield drop, as shown in Fig. 4b, on first loading. Thus in this case the load borne by the composite after failure of the fibre–matrix interface was less than just before the interface failed. This contrasted with the behaviour of the composite with the unetched fibres where the yield drop was either very small or non-existent. The sensitivity of the composites to the condition of the fibre–matrix interface was also reflected in the pull-out tests which showed similar behaviour. Unfortunately the stress distribution in these tests is not simple, and failure of the fibre–matrix interface occurred under the tensile stresses at the ends of the cylinder so that realistic estimates of the shear strength of the fibre–matrix interface were not possible.

In the imposed strain controlled cyclic tests at 0.83 Hz the hysteresis loops of the well-bonded fibre composites were asymmetric, both the mean force and displacement lying outside the loop itself, as shown in Fig. 5. Consequently the stiffness of the composite was not constant, but an average stiffness had to be defined as

$$k_{\text{mean}} = \frac{1}{2x_{\text{m}}} \int_{-x_{\text{m}}}^{x_{\text{m}}} k\,\mathrm{d}x = \frac{1}{2x_{\text{m}}} [P(x)]_{-x_{\text{m}}}^{x_{\text{m}}} \quad (1)$$

where x_{m} is the displacement amplitude and k the stiffness and $P(x)$ the force. The mean stiffness is then just the slope of the line joining the ends of the loop. Other methods of averaging such as taking a mean strain energy lead to a similar conclusion. The specific damping is calculated by taking the strain energy as $\frac{1}{2}k_{\text{mean}}x_{\text{m}}^2$ and is given in Fig. 6.

Unlike the composites with no interfacial slip, the composites in which interfacial slip was promoted showed almost elliptical loops in which the energy loss per cycle was very much greater than the composites without slip, (Fig. 7) and this resulted in an increase in the specific damping of the composites with slip compared to those without (Fig. 6). In the slow tensile tests, even though complete interfacial failure occurred, the com-

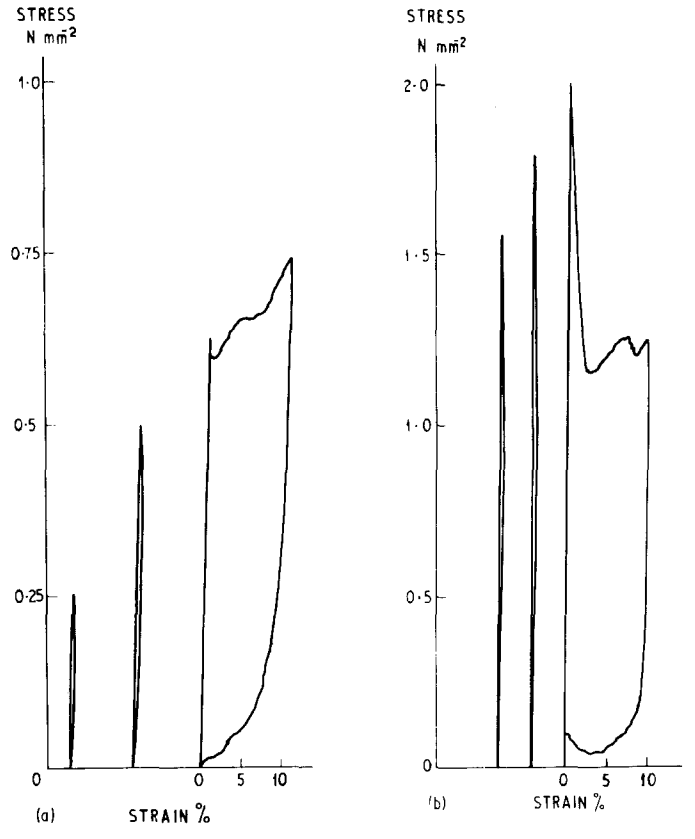

Figure 4 (a) Stress–strain loops of a composite made of unetched fibres, showing interfacial slip. (b) Stress–strain loops of a composite made of etched fibres, showing a yield drop and subsequent interfacial slip.

posites were capable of sustaining a static load almost indefinitely, apart from a slight viscoelastic relaxation of the matrix. However during cyclic testing with an increasing strain amplitude, or prolonged testing at one amplitude, the mean load borne by the composites with slip fell with each cycle until a limiting value was reached. On decreasing the amplitude this limiting mean load was maintained as shown in Fig. 8. On increasing the amplitude again the mean load stayed at the lower level. The transient effect of the fall in mean load was accompanied by slight increase in the dynamic stiffness as measured by the slope of the hysteresis loop, and a decrease in the energy lost per cycle.

In the forced vibration tests the effect of interfacial slip can be seen on the resonance curves of Fig. 9. Very much larger exciting forces were required to produce the same amplitude of vibration in composites exhibiting interfacial slip than in those which did not. This was consistent with the significantly higher damping in the material with slip, and also accounts for the greater width of the resonance curves. A direct comparison of the properties of the silicone rubber with and without fibre reinforcement was not possible,

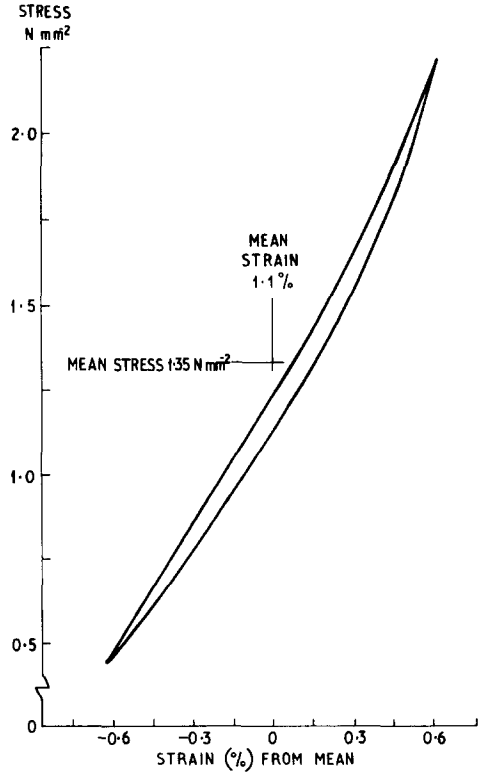

Figure 5 Hysteresis loop of a composite without interfacial slip, tested at 0.83 Hz.

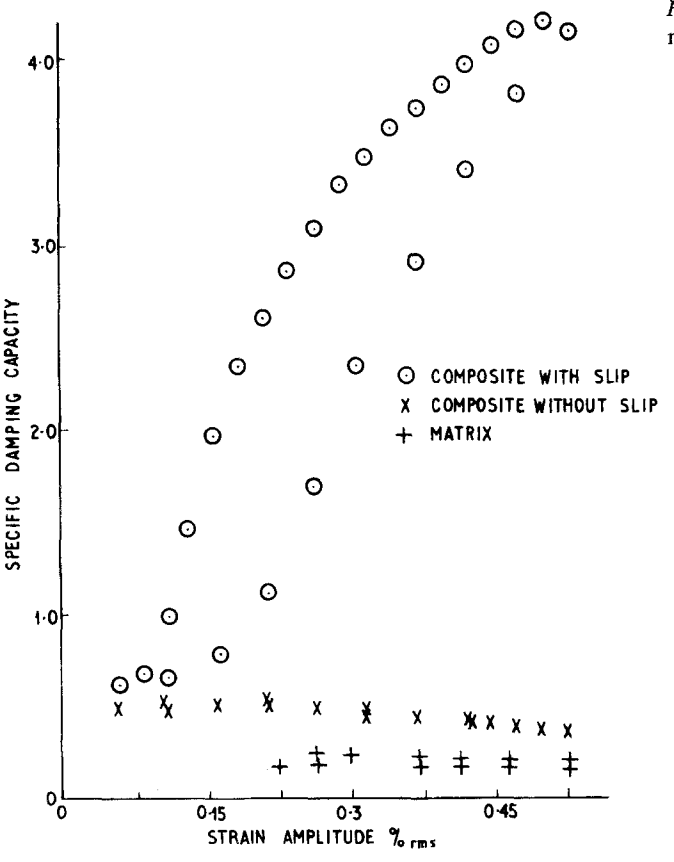

Figure 6 The specific damping capacities of the materials tested at 0.83 Hz.

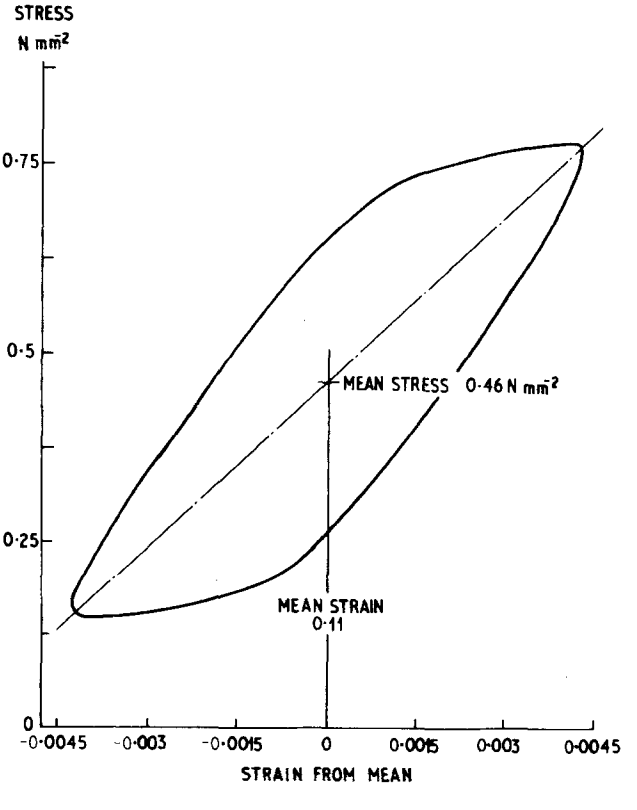

Figure 7 Hysteresis loop of a composite with interfacial slip at 0.83 Hz.

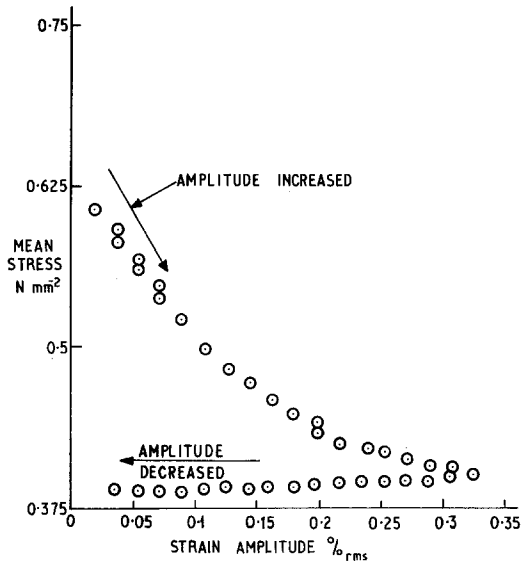

Figure 8 The effect of vibration on the mean stress borne by a composite with interfacial slip.

however, due to the difficulty in making comparisons at similar frequencies, in view of the marked difference in elastic modulus of the two materials.

4. Discussion

4.1. Tensile behaviour

Fibre reinforcement is widely used to increase the elastic moduli of polymers: in this case Young's modulus of all the composites was increased from $3\,N\,mm^{-2}$ to $200\,N\,mm^{-2}$, before failure of the fibre–matrix interface occurred. This may be compared with the values of $164\,N\,mm^{-2}$ and $120\,N\,mm^{-2}$ calculated from the theories developed by Kelly [5] and Mileiko [6] respectively. However agreement with either theory is not good enough for preferring one model since the main source of error is the non-linear elastic behaviour of the matrix at the relatively large local shear strains near the fibres.

The initial elastic behaviour of the composites with weak fibre–matrix interfaces was terminated by failure of the interface followed by interfacial slip. In the case of the etched fibres the shear strength of the fibre–matrix interface was initially greater than the shear stress to produce sliding, thus leading to a marked yield drop as the load borne by the fibres decreased suddenly, although on retesting there was no yield drop as the shear stress to restart sliding was similar to that required to continue sliding. In the composites with unetched fibres the shear strength of the interface

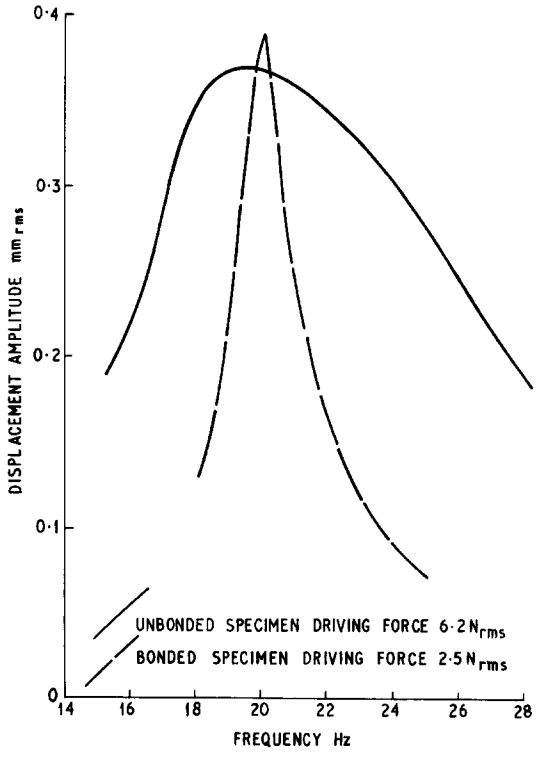

Figure 9 The resonance curves of composites with and without interfacial slip.

and the frictional sliding stress were always similar so that no yield drop occurred. It is the mechanism of slip in composites in which the interfacial shear stress to start sliding is similar to that to continue sliding, that is pursued in more detail.

The simplest criterion for the initial failure of the interface is that of a critical interfacial shear stress τ_{crit}. For simplicity it is convenient to develop the case of a rigid fibre, although by a comparison of available elastic inclusion solutions the difference between the stress distribution around inclusions whose modulus is very much greater than that of the matrix and the limiting case of the rigid inclusion, is small. Following the line of argument by Cox [7], the axial load in the fibre, P, may be taken to build up from the ends according to

$$\frac{dP}{dx} = -K(w-z) \qquad (2)$$

Here w is the axial displacement of a point which is a distance x from a fibre end, the point being in the matrix and distant from the fibre. Similarly z is the axial displacement of a corresponding point on the matrix side of the fibre–matrix inter-

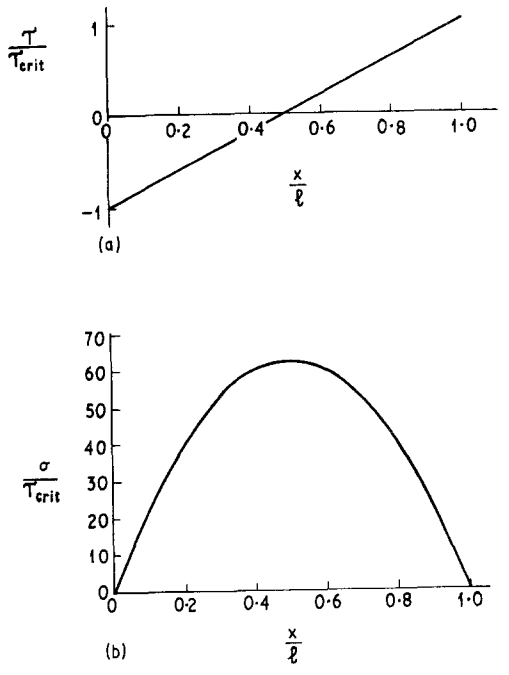

Figure 10 (a) The shear stress distribution on the interface just before slip starts ($e = e_{crit}$). (b) The tensile stress distribution on the fibre just before slip starts.

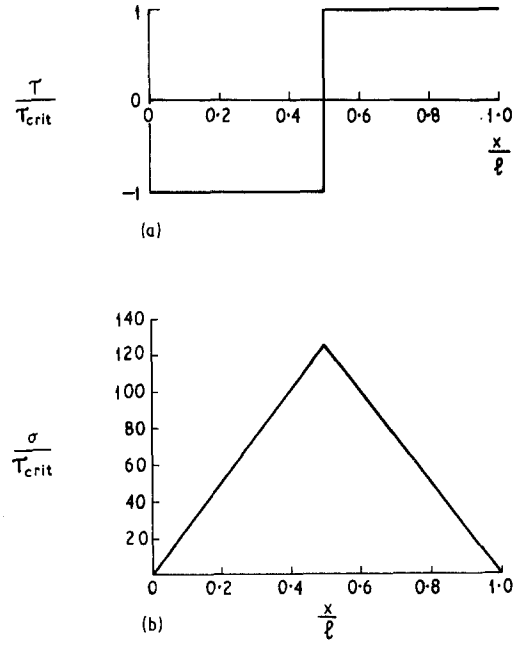

Figure 11 (a) The shear stress distribution on the fibre-matrix interface after extensive interfacial slip ($e = e_{max}$). (b) The tensile stress distribution in the fibre after extensive interfacial slip ($e = e_{max}$).

face. When the interface is intact z is zero, but during subsequent interface failure and slip $dw/dz = 1$. Differentiating Equation 2 and remembering that dw/dx is the matrix strain e, and dz/dx is the fibre strain, which is zero for a rigid fibre, leads to $d_2P/dx^2 = -Ke$. Integrating this twice employing the boundary conditions that $dP/dx = 0$ at $x = l/2$ and $P = 0$ at $x = 0, l$ gives

$$P = \frac{Ke}{2}(lx - x^2). \tag{3}$$

By considering the axial equilibrium of an element of fibre, the interfacial shear stress before failure of the interface is

$$\tau = -\frac{Ke}{4\pi r}(l - 2x) \tag{4}$$

Let interfacial slip start at a critical value $|\tau_{crit}|$ so that the tensile strain e_{crit} to start interface sliding is $(4\pi r\,\tau_{crit}/Kl)$. After sliding has started a reasonable first approximation is that the limiting interface shear stress is constant, so that the distance x' over which slip occurs is $\frac{1}{2}(l - 4\pi r\,\tau_{crit}/Ke)$, for e greater than the critical value e_{crit} to start sliding. The load at the fibre centres when there is sliding over $0 \leqslant x < x'$ and no sliding over $x' < x \leqslant l/2$ is

$$P(l/2) = \pi r\,\tau_{crit} l(1 - e_{crit}/2e) \tag{5}$$

As the imposed strain increases the load tends asymptotically to $\pi r\,\tau_{crit}$ which is the load borne when the interface is completely broken, as long as the fibre length is less than $(E_f e r/\tau_{crit})$. The shear stress and axial load distributions corresponding to these cases are shown in Figs. 10 and 11. The load borne by the matrix may be added to that borne by the fibres, and on this basis the slope of the stress–strain curve should reduce rapidly to $(1 - f)E_m$ where f is the volume fraction of fibres, as any increase in load is borne by a tensile strain in the matrix. Experimentally, however, the modulus of this part of the stress–strain curve is significantly greater than that of the matrix alone, and it is appropriate to reconsider one of the earlier simplifying assumptions.

It was originally assumed that the interfacial shear stress during sliding was constant, but in fact this stress must increase since the radial stress across the interface also increases with strain due to the transverse contraction of the matrix onto the fibres. This problem may be treated simply by imagining that a fibre is removed from the matrix after a strain $e, (e \gg e_{crit})$, and solving for the radial stress necessary to enlarge the hole so that it fits the fibre once more. This is, of course, an adaptation of the well-known shrink fit problem

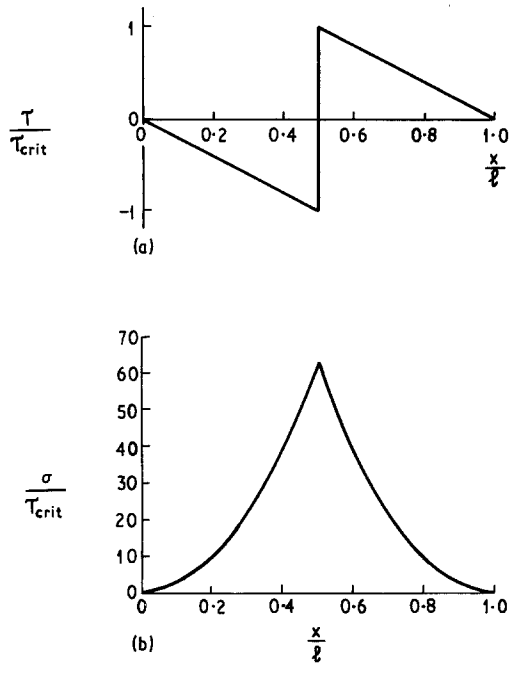

Figure 12 (a) The shear stress distribution on the interface during unloading ($e = e_{max} - e_{crit}$). (b) The tensile stress in the fibre during unloading ($e = e_{max} - e_{crit}$).

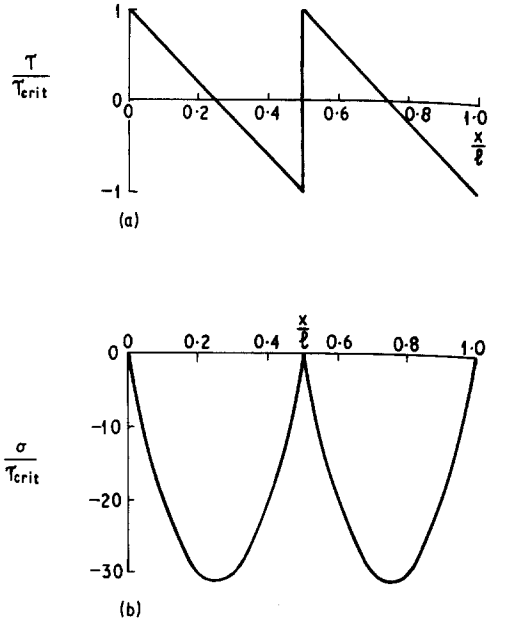

Figure 13 (a) The shear stress distribution on the interface during unloading ($e = e_{max} - 2e_{crit}$). (b) The tensile stress in the fibre during unloading ($e = e_{max} - 2e_{crit}$).

and the radial stress (σ_r) is related to the axial sliding strain e by

$$\sigma_r = \frac{E_m e}{3}\left(\frac{r^2}{R^2} - 1\right) \qquad (6)$$

where the Poisson's ratio is $\frac{1}{2}$. E_m is the Young's modulus of the matrix and R and r are the fibre spacing and radius.

Using the usual frictional law ($\tau = \mu\sigma_r$) where μ is the coefficient of friction shows that the limiting interfacial shear stress (τ_{crit}) increases linearly with strain as long as the difference between true and engineering strain is small. On this basis the stress–strain curve is compared with that predicted theoretically using a value of 0.091 N mm^{-2} for the initial value of τ_{crit} and $\mu = 0.13$ in Fig. 14. It may however be noted that it has been assumed that all the fibre–matrix interfaces break at the critical value of the interfacial shear stress, neglecting any statistical variations. It is however quite likely that this is not the case, and a contribution

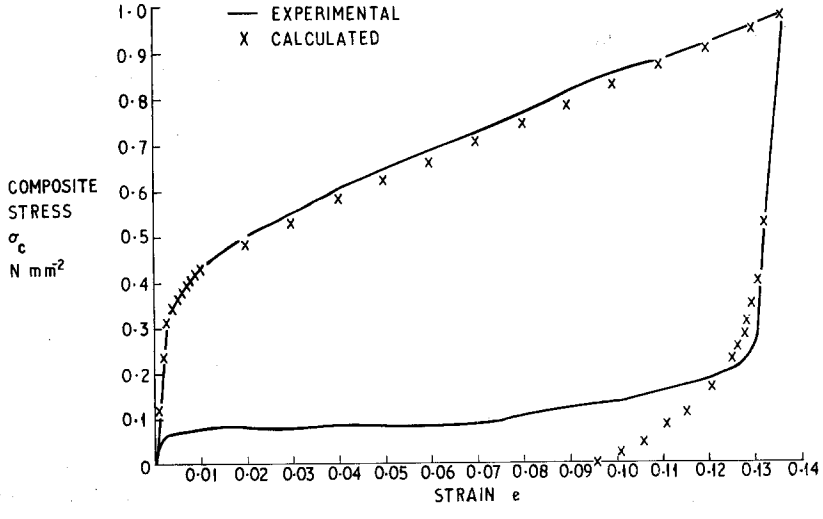

Figure 14 A comparison of an observed hysteresis loop with interfacial slip, with that calculated using $\tau_{crit} = 0.09$ N mm^{-2}.

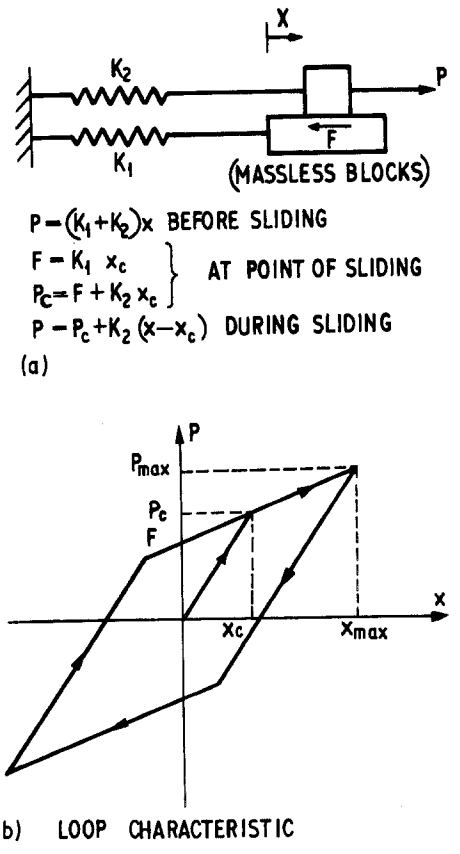

Figure 15 Bi-linear hysteresis model.

to the secondary modulus will arise from fibres whose interface is still intact.

On unloading the composites, interfacial slip stops initially, and both the fibres and the matrix are unloaded so that the modulus of this part of the cycle must be the same as that of the first part. To examine the unloading part of the cycle use may be made of the ability to superimpose elastic solutions until interfacial slip occurs, when the boundary conditions change. Thus superimposing the fibre and interface stress distributions corresponding to a compressive applied load without fibre buckling or interfacial slip (i.e. the Cox stress distribution with the signs reversed) effectively unloads the composite. If Fig. 11 shows the stress distribution in the fibres at the maximum strain in the cycle (e_{max}), on decreasing the strain to ($e_{max} - e_{crit}$) the stress distribution becomes that shown in Fig. 12

$$\tau = -2\tau_{crit}\, x/l \quad 0 \leqslant x < l/2 \qquad (7)$$

$$= 2\tau_{crit}(1 - x/l) \quad l/2 < x \leqslant l \qquad (8)$$

$$\sigma = 2\tau_{crit} x^2/rl \quad 0 \leqslant x \leqslant l/2 \qquad (9)$$

$$\sigma = 2\tau_{crit}(l-x)^2/rl \quad l/2 \leqslant x \leqslant l \qquad (10)$$

On further unloading to ($e_{max} - 2e_{crit}$) the stress distributions becomes as shown in Fig. 13 in which

$$\tau = \tau_{crit}(1 - 4x/l) \quad (0 \leqslant x < l/2) \qquad (11)$$

$$\tau = \tau_{crit}(3 - 4x/l) \quad (l/2 < x \leqslant l) \qquad (12)$$

$$\sigma = 2\tau_{crit} x(2x - l)/rl \quad (0 \leqslant x \leqslant l/2) \qquad (13)$$

$$\sigma = 2\tau_{crit}(x - l)(2x - l)/rl \quad (l/2 \leqslant x \leqslant l) \qquad (14)$$

It should be noted that the tensile stress is zero at the fibre ends and also at the centre of the fibre but is compressive elsewhere. At this point interface sliding should start to occur in the reverse direction. The superposition principle could be extended in an approximate way to deal with this if the interfacial shear stresses are once again truncated at $|\tau_{crit}|$ as in the loading cycle. This leads to the stress–strain cycle shown in Fig. 14 in which the modulus of the stress–strain curve in both forward and reverse slip is similar as in the classical models of bi-linear hysteresis (Fig. 15).

However an examination of the stress distributions of Figs. 12 and 13 indicates that it is perhaps not surprising that reverse slip does not occur in the simple stable manner of forward slip. At the fibre centres and ends the load in the fibres is zero so that in the cross-sections of the composite containing the fibre centre and ends the tensile load is borne only by matrix. However at $x/l = \frac{1}{4}$ and $\frac{3}{4}$, a compressive load develops in the fibres so that the matrix must necessarily bear a larger tensile load such that the load borne by each cross-section is the same. Thus instead of sliding occurring in a stable manner it seems likely that the onset of sliding would be a catastrophic event in which complete internal stress redistribution could occur such that the fibres could shed compressive load and the matrix tensile load without the externally applied load changing, thus minimizing the total strain energy in the system. The alternative explanation is that as the fibres become loaded in compression fibre buckling occurs and this process initiates stress redistribution by interfacial slip. The fibre buckling analyses which exist [9] deal with two-dimensional models of continuous fibres and are upper-bound calculations, and are thus of limited applicability. However these suggest that the compressive loads in the fibres needed to cause buckling are an order of magnitude greater than those observed experimentally. However this is an academic point for

the composites in which sliding occurs readily, as reverse slip occurs when the interface shear stress reaches the critical value. This also corresponds to the point where the fibres just start to bear axial compressive loads along their whole length. For the composites with the etched fibres, higher interface shear stress are required to cause sliding and larger compressive loads can be borne by the fibres before reverse sliding occurs. Thus when slip occurs during unloading such that the fibre sheds its compressive load, the tensile load borne by the composite as a whole increases, and this leads to the curious effect of a negative modulus. That is to say, the specimen gets shorter but bears an increased tensile load, as the compressive load borne by fibres is relieved by interface slip. Because reverse slip leads to a complete internal stress re-distribution the fibres did not usually bear large compressive loads during unloading and the hysteresis loops generally returned to the origin. However when very large tensile strains were imposed in loading the composites where often left with a permanent set at zero load, such that significant compressive loads were left in the fibres unrelieved by slip. In such cases the yield stress in the subsequent cycle was increased as the marked residual stress distribution had to be cancelled by the new tensile loading.

4.2. Dynamic behaviour

Dynamic tests were performed on the composites in both imposed sinusoidal displacement and force tests. In these tests it is again useful to relate the properties of the matrix alone with those of the bonded composites before proceeding to discuss the effect of interfacial slip.

In the absence of interfacial failure the energy loss in the composites is purely viscoelestic and comes from the matrix. If the material were linearly viscoelastic the storage and loss moduli of the composite would be greater than that of the matrix by the same factor, which would depend on the fibre distribution.

On the basis of Mileiko's [6] model in which load is transmitted from fibre to fibre through a series of hinges, the ratio of the shear strain in the hinges to the imposed tensile strain is equal to the ratio of the fibre overlap to spacing. In the present case, this is a factor of 23. Thus at the same imposed amplitude of vibration, more energy is stored elastically, and more energy is dissipated in the composite than in a specimen of matrix alone.

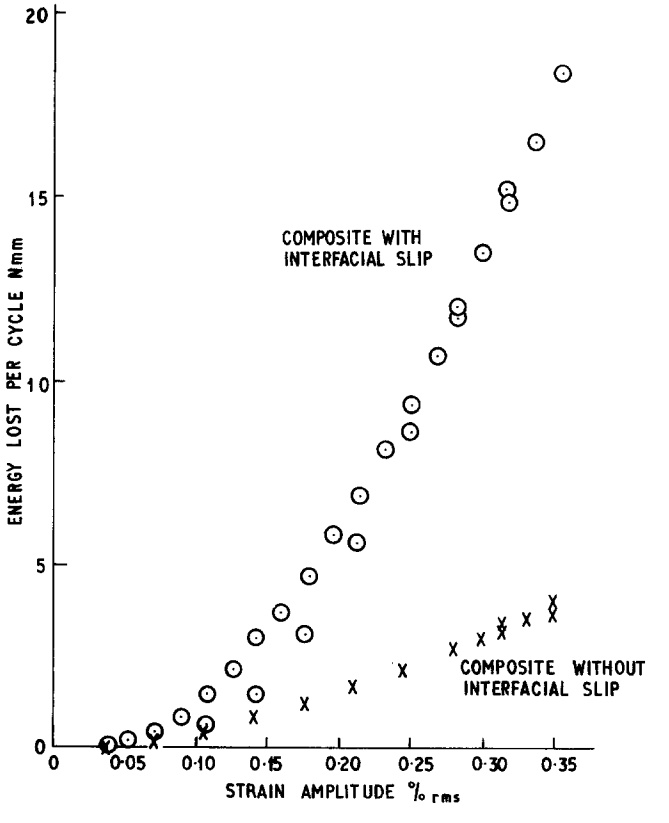

Figure 16 A comparison of the energy loss of a composite with interfacial slip with one not exhibiting slip.

The specific damping capacity, the ratio of the energy stored to that dissipated, is comparable to that of the matrix alone. However, the specific damping capacities of the composites without interfacial slip were often 2 or 3 times greater than for the matrix alone, and this may be accounted for largely by the non-linear nature of the matrix at the relatively large shear strains developed near the fibres. The stiffness of the bonded composites was approximately 30 times that of the matrix alone, while the energy loss per cycle at similar overall strains was 50 to 80 times greater in the composites than the matrix.

The energy loss was, however, very much greater in the composites exhibiting interfacial slip than those showing only viscoelastic energy loss as shown in Fig. 16, although at low amplitudes where slip did not occur the energy loss in both types of material was similar. In comparison, the viscoelastic energy loss from a specimen of matrix alone would be negligible. Energy loss in these composites occurs by interfacial sliding over a length x' which increases with amplitude. The increment of energy dE per fibre which is dissipated on increasing the strain from e to $e + de$ is $2\pi r \tau_{crit} x'^2 de$. Now x' is given by $1/2(l - 4\pi r \tau_{crit}/Ke)$ so that the energy lost per fibre in starting a cycle at zero strain and increasing the strain to $2\Delta e$ is

$$\int_{e_{crit}}^{2\Delta e} \frac{1}{2} \pi r \tau_{crit} (l - 4\pi r \tau_{crit}/Ke)^2 de.$$

Unfortunately reverse sliding is not as simple as forward sliding, but as a simple estimate assume that the energy lost in the first half of the cycle is the same as that in the second half. On this basis frictional energy dissipation should start at a critical strain, e_{crit}, and the energy loss should increase with the strain amplitude Δe until the whole interface is sliding when the energy loss should approach $2\pi r \tau l^2 \Delta e$. The predicted energy loss is compared with that observed using the same value of τ_{crit} as in the tensile test and taking K as $2\pi G_m \ln(R/r)$ as suggested by Kelly [5]. The agreement is encouraging for such a simple model, as shown in Fig. 17.

Turning now to the use of the material in a simple resonating system, the frequency at resonance is determined by the stiffness of the material and the vibrating mass. In a perfectly elastic system with no energy loss the vibration amplitude of resonance would increase with each cycle, but in practice the damping inherent in practical systems limits the amplitude. A simple comparison of the properties of the matrix and the composites without slip is difficult as the difference in elastic moduli prevents a comparison being made at the same resonant frequency. However this problem does not arise in examining the effect of interfacial slip. The main features of the material response in slow tensile and cyclic testing also occur in resonance at 20 Hz. The energy loss per cycle was again markedly higher when interfacial slip occurred, and significantly larger forces were required to excite amplitudes of vibration comparable to those in the absence of slip. However as interfacial slip

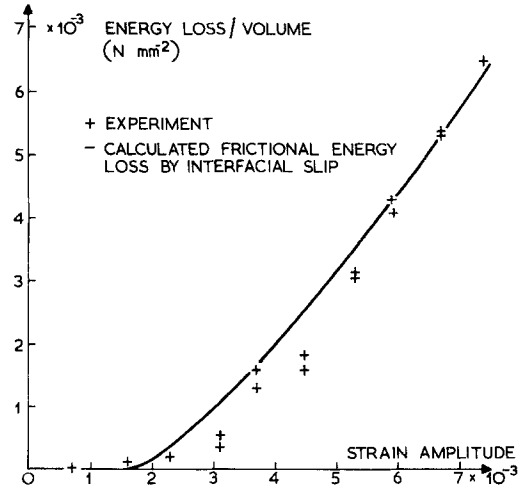

Figure 17 The frictional energy lost per cycle compared with that predicted.

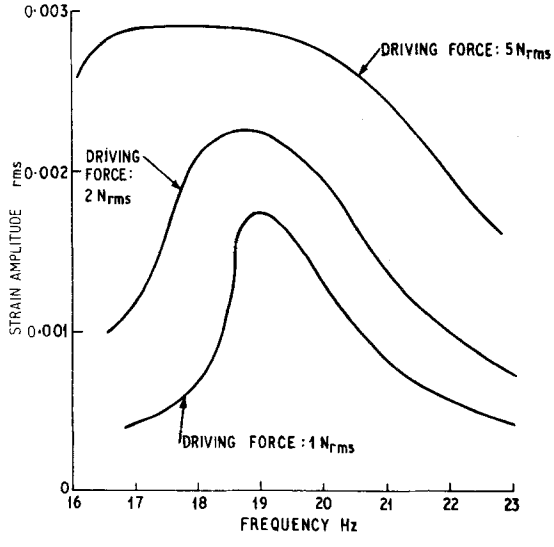

Figure 18 Resonance curves of a composite with interfacial slip showing the increasing asymmetry of the curves with amplitude.

only occurs above a critical amplitude, at small amplitudes the energy loss and stiffness were comparable to the bonded composites.

Frictional damping is however non-linear and increases with increasing amplitudes, and this, which is a useful response for a structural material, is reflected in the increasing width and asymmetry of the resonance curves (Fig. 18).

Although the use of interfacial slip shows promise as a way of developing composites with high damping, slip also unfortunately affects the load-bearing capacity of the composite with a superimposed vibration. Although in slow tensile tests the composites with slip were able to sustain a static load almost indefinitely, the effect of a superimposed vibration is to cause a marked fall in the mean load borne by the composite. This is consistent with stress redistribution during reverse slip such that the interfacial shear stress is completely relieved, the load borne by the fibres becomes zero and all the load is borne by the matrix in tension. Thus in Fig. 8 the mean stress which would be borne by the matrix in tension at a strain of 11% is $0.35\,N\,nm^{-2}$ and this corresponds well to the limiting value to which the stress borne by the composite falls before becoming constant. This feature prevents the dynamic properties being correlated with a simple bi-linear hysteresis model such as that developed by Caughey [8]. However, much more important, is that this prevents the use of composites with large amounts of interface slip being used to damp vibration in critical components where the ability to sustain a high mean load is important. There are many much less critical components, such as the internal non-structural panels of aircraft and motor cars where the high damping capacity could be used to damp vibration in components which would only bear relatively low mean loads. Such composites would have short fibres with a length less than $(\sigma_f r/\tau_{crit})$, σ_f being the fibre fracture stress, such that sliding could occur over the whole length, the critical strain at which interfacial slip starts being controlled by the strength of the interface. The frictional sliding stress could also be controlled through the shrinkage of the matrix onto the fibres. Such composites, which would contain higher volume fractions of fibres than used in this work, would also appear to have a useful fracture toughness, in that the fibres should all pull out of the matrix rather than break during failure, thus absorbing significant amounts of energy. The increase in damping and the corresponding decrease in dynamic modulus when interfacial slip starts show promise for the non-destructive testing of more conventional composites, particularly if the energy lost per cycle can be correlated with the extent of interfacial damage as suggested by Fig. 17.

5. Conclusions

Interfacial slip has been shown to have a marked effect on the stress–strain behaviour of fibre composites and this has been interpreted using a simple model of interfacial slip. This has allowed the energy lost per strain cycle to be correlated with the extent of interfacial damage and indicates the way in which interfacial slip can be used to produce composites with a useful degree of damping.

References

1. D. McLEAN and B. E. READ, *J. Mater. Sci.* **10** (1975) 481.
2. Z. HASHIN, *Int. J. Solid Struct.* 6 (1970) 797.
3. R. D. ADAMS and D. G. C. BACON, *J. Comp. Mater.* 7 (1973) 53.
4. D. J. NELSON, *J. Sound and Vibration* (Submitted).
5. A. KELLY, "Strong Solids" (Oxford University Press, 1966).
6. S. T. MILEIKO, *J. Mater. Sci* 5 (1970) 254.
7. H. L. COX, *Brit. J. Appl. Phys.* 3 (1952) 72.
8. T. K. CAUGHEY, *J. Appl. Mech.* 27 (1960) 640.
9. B. W. ROSEN, "Fibre Composite Materials," (American Society for Metals, Metals Park, Ohio, 1964).

Received 30 September and accepted 14 December 1977.